

University of Groningen

## Catalytic and kinetic mechanism of epoxide hydrolase

Rink, Rick

**IMPORTANT NOTE: You are advised to consult the publisher's version (publisher's PDF) if you wish to cite from it. Please check the document version below.**

*Document Version*

Publisher's PDF, also known as Version of record

*Publication date:*

1999

[Link to publication in University of Groningen/UMCG research database](#)

*Citation for published version (APA):*

Rink, R. (1999). *Catalytic and kinetic mechanism of epoxide hydrolase*. s.n.

### Copyright

Other than for strictly personal use, it is not permitted to download or to forward/distribute the text or part of it without the consent of the author(s) and/or copyright holder(s), unless the work is under an open content license (like Creative Commons).

The publication may also be distributed here under the terms of Article 25fa of the Dutch Copyright Act, indicated by the "Taverne" license. More information can be found on the University of Groningen website: <https://www.rug.nl/library/open-access/self-archiving-pure/taverne-amendment>.

### Take-down policy

If you believe that this document breaches copyright please contact us providing details, and we will remove access to the work immediately and investigate your claim.

Downloaded from the University of Groningen/UMCG research database (Pure): <http://www.rug.nl/research/portal>. For technical reasons the number of authors shown on this cover page is limited to 10 maximum.

## Summary and Concluding Remarks

Epoxide hydrolase from *Agrobacterium radiobacter* AD1 catalyzes the hydrolysis of epoxides to their corresponding vicinal diols without the use of a cofactor. The enzyme is involved in the degradation of epichlorohydrin and 1,3-dichloro-2-propanol, enabling the organism to grow on these compounds as the sole source of carbon and energy (van den Wijngaard et al., 1989). The 34 kDa enzyme was purified from *A. radiobacter* AD1 and the N-terminus, an internal fragment, and the C-terminal fragment were sequenced by Edman degradation (Jacobs et al., 1991). The enzyme hydrolyzes a wide variety of terminal epoxides and epichlorohydrin is the best substrate, indicating that this epoxide hydrolase is specially adapted for the hydrolysis of this compound (Jacobs et al., 1991). Only mammalian epoxide hydrolase genes were cloned and characterized when the work described in this thesis started, and little was known about the catalytic mechanism. The aim of the work of this

thesis was to obtain insight in the catalytic and kinetic mechanism of the epoxide hydrolase from *A. radiobacter* AD1.

### *Cloning and Expression of Epoxide Hydrolase*

The gene coding for epoxide hydrolase was cloned from *A. radiobacter* AD1 by means of the polymerase chain reaction (PCR). Degenerated primers were based on the known amino acid sequences of the N- and C-terminus of the enzyme. The gene was cloned in the expression vector pGEF+ which was constructed earlier for the overexpression of haloalkane dehalogenase from *Xanthobacter autotrophicus* GJ10 in *Escherichia coli* (Schanstra et al., 1993). The recombinant epoxide hydrolase was produced up to 40% of the total cellular protein content of *Escherichia coli* BL21 (DE3) and could easily be purified using a two-step purification procedure. The high expression levels of epoxide hydrolase made it possible to perform the rapid-quench

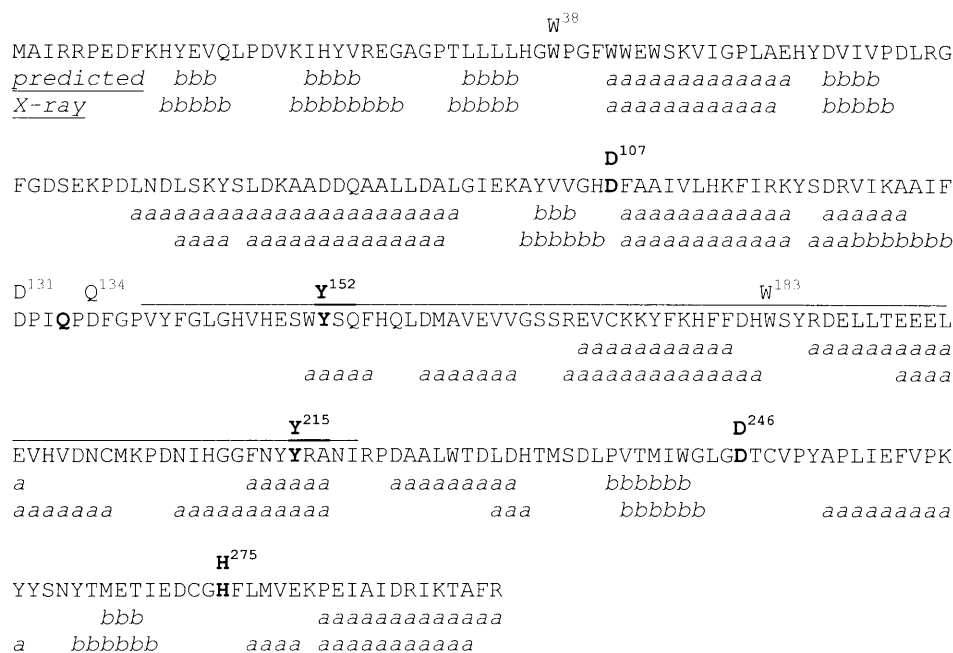


**Figure 1.** Amino acid sequence and secondary structure elements of the epoxide hydrolase from *Agrobacterium radiobacter* AD1. The secondary structure elements are shown below the residues as *a* for an  $\alpha$ -helical residue and *b* to indicate residues that are part of a  $\beta$ -strand. The residues that are part of the cap domain are overlined. The catalytic residues that were identified by site-directed mutagenesis are shown in bold and their position in the sequence are shown in superscript. Other residues that are discussed are also shown.

experiments that are described in *Chapters 2* and *3*, since gram amounts of pure enzyme were needed in these experiments.

The epoxide hydrolase gene (*echA*) codes for an enzyme of 294 amino acids with the expected molecular weight. An identical epoxide hydrolase gene was obtained from the closely related strain *A. radiobacter* CFZ11 by subcloning from a 2.3-kilobase fragment of chromosomal DNA on which the gene was located. The same DNA fragment is also present in strain AD1 as is shown by Southern blot analysis with a probe for the epoxide hydrolase gene. Downstream of the epoxide hydrolase gene an open reading frame encoding the first 34 amino acids of a possible haloalcohol dehalogenase was found. Both enzymes were simultaneously expressed in strain

AD1 when induced with epichlorohydrin, indicating that these genes are part of an operon (van den Wijngaard et al., 1989). The whole gene encoding the hypothetical haloalcohol dehalogenase has now been cloned and expressed in *E. coli*. The encoding enzyme indeed has haloalcohol dehalogenase activity (J.E.T. van Hylckama Vlieg, personal communication).

The *echA* gene from *A. radiobacter* AD1 was the first bacterial epoxide hydrolase gene to be cloned (Rink et al., 1997). Another bacterial epoxide hydrolase gene has been obtained from *Corynebacterium* sp. and the encoded enzyme shares 30% sequence identity with the epoxide hydrolase from *A. radiobacter* AD1 (Misawa et al., 1998). A third bacterial epoxide hydrolase gene was recently cloned from *Rhodo-*

*coccus* encodes is not hydrolas new type al., 1998

A ho bases w epoxide l resulted epoxide l fold enzy epoxide l they pro ancestor. alkane de GJ10 and *tomyces a* three-dim ly indica hydrolase family. E obtained tions base from circu showed al hydrolase Recently, hydrolase solved and hydrolase 1999). The epoxide hy structure a with the reported in tural elem predicted v Sequenc between  $\alpha$  are restrict topology. occupy pre acid sequer identified by

*coccus erythropolis* DCL14. This gene encodes a small protein of 16.4 kDa, and it is not similar to any known epoxide hydrolase, making it the first example of a new type of epoxide hydrolase (Barbarito et al., 1998).

A homology search in sequence databases with the amino acid sequence of epoxide hydrolase from *A. radiobacter* AD1 resulted in hits with all the eukaryotic epoxide hydrolases and many  $\alpha/\beta$ -hydrolase fold enzymes. The bacterial and eukaryotic epoxide hydrolases are clearly related and they probably evolved from a common ancestor. Sequence similarities with haloalkane dehalogenase from *X. autotrophicus* GJ10 and bromoperoxidase A2 from *Streptomyces aureofaciens*, enzymes of which the three-dimensional structure is known, clearly indicate that the strain AD1 epoxide hydrolase belongs to the  $\alpha/\beta$ -hydrolase fold family. Experimental support for this was obtained from secondary structure predictions based on the amino acid sequence and from circular dichroism spectroscopy, which showed almost identical spectra for epoxide hydrolase and haloalkane dehalogenase. Recently, the X-ray structure of epoxide hydrolase from *A. radiobacter* AD1 was solved and it indeed shows the typical  $\alpha/\beta$ -hydrolase fold structure (Nardini et al., 1999). The secondary structure elements of epoxide hydrolase that are obtained from the structure are shown in Figure 1 together with the predicted secondary structure reported in Chapter 2. Especially the structural elements of the main domain were predicted very well.

Sequence similarities are generally low between  $\alpha/\beta$ -hydrolase fold enzymes and are restricted to specific areas within the topology. The catalytic triad residues occupy preserved positions in the amino acid sequence and can therefore easily be identified by sequence alignments.

#### Catalytic Mechanism

The catalytic mechanism of epoxide hydrolase is depicted in Figure 2, together with the catalytic residues. The catalytic triad residues Asp107, His275, and Asp246 were identified by sequence alignments with other  $\alpha/\beta$ -hydrolase fold enzymes. Replacement of these residues by Ala/Glu, Arg/Gln, and Ala, respectively, resulted in mutant enzymes which had completely lost the capacity to hydrolyze epichlorohydrin. The D246A mutant was an exception since it retained 0.4% of the wild-type activity and this led to the suggestion that Asp131 partially compensates for the loss of Asp246. The X-ray structure of epoxide hydrolase confirmed the presence of the postulated catalytic triad residues in the active site as well as a possible role for Asp131 in catalysis. Furthermore, the structure showed that Tyr152 and Tyr215, which reside in the  $\alpha$ -helical cap domain, are pointing into the active site. Results described in Chapters 4 and 5 show that these tyrosines are involved in catalysis by serving as proton donor.

Based on the structural and mutagenesis studies, epoxide hydrolysis is proposed to proceed as follows. In the Michaelis complex, the epoxide substrate is bound in the active site of epoxide hydrolase by hydrogen bonds between the oxirane oxygen and the hydroxyl groups of Tyr152 and Tyr215. The alkylation half-reaction is the first part of the catalytic cycle and it involves the nucleophilic attack of Asp107 on the least-hindered carbon atom of the oxirane ring to form a covalent intermediate, also called the alkyl enzyme (Figure 2A). The occurrence of an alkyl-enzyme intermediate was shown in Chapter 2 by a single-turnover experiment with the H275R mutant of epoxide hydrolase in which the ester intermediate could be trapped. The nucleophilic attack of Asp107 is facilitated

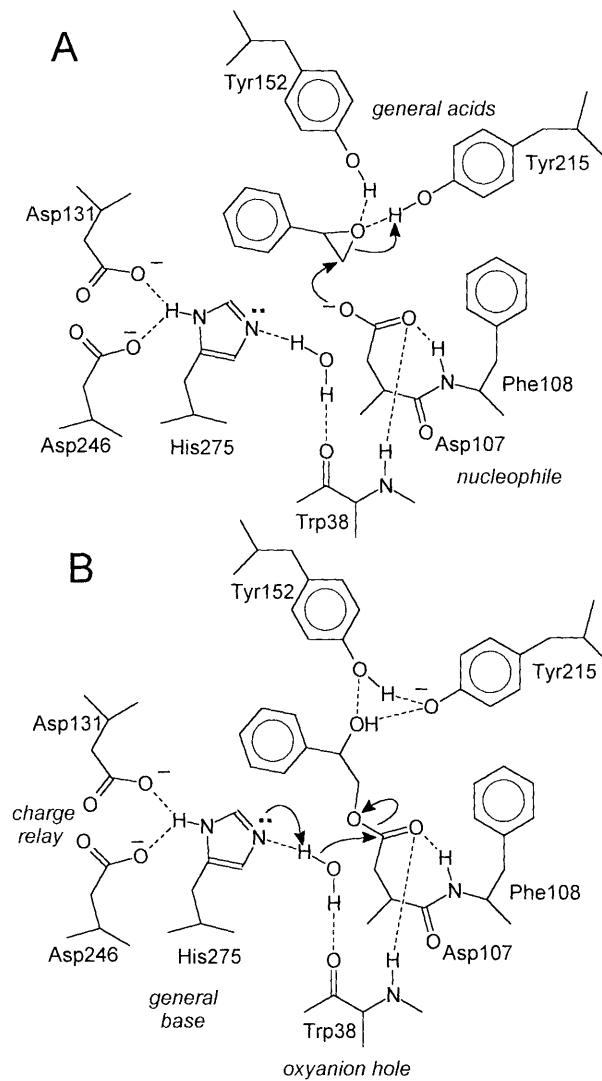


**Figure 2.** Reaction mechanism of the epoxide hydrolase from *Agrobacterium radiobacter* AD1. (A), alkylation half-reaction, (B), hydrolytic half-reaction.

by the Tyr152 and Tyr215 residues, which activate the substrate by acting as general acids. Consequently, the alkyl-enzyme intermediate is protonated by one of the tyrosine residues yielding a stable covalent intermediate and a tyrosinate.

The hydrolytic half-reaction is the second catalytic step and it involves product release

(Figure 2B). The general base His275 abstracts a proton from a well-positioned water molecule and it is assisted by the charge relay residues Asp246 and Asp131. The activated water molecule attacks the carbonyl group of the covalent intermediate to hydrolyze the ester bond and to form the diol. The transition state of this hydrolysis

reacti  
on the  
by an  
backb  
and P  
struct  
sequ  
conser  
hydro  
among

A s  
found  
Site-di  
micro  
soluble  
catalyt  
base-cl  
Glu404  
pective  
al., 19  
1996 a  
et al.,  
an alk  
alignm  
idues T  
hydroly  
in the s  
and ma  
ly indi  
also ce  
hydroly  
a few  
among  
sugges  
micro  
and T  
hydroly  
assist  
proton  
ments  
these t  
of the  
The  
somal  
instea  
bacter

reaction in which a negative charge develops on the carboxylic oxygen atom is stabilized by an oxyanion hole, that is formed by the backbone amide nitrogen atoms of Trp38 and Phe108 as is evident from the crystal structure. Trp38 is part of the oxyanion sequence HGWP and it is absolutely conserved as HGxP among epoxide hydrolases and almost fully conserved among other  $\alpha/\beta$ -hydrolase fold enzymes.

A similar catalytic mechanism has been found for the eukaryotic epoxide hydrolases. Site-directed mutagenesis studies with rat microsomal epoxide hydrolase and mouse soluble epoxide hydrolase identified the catalytic triad residues (nucleophile-general base-charge relay) as Asp226-His431-Glu404 and Asp333-His523-Asp495, respectively (Bell and Kasper, 1993; Borhan et al., 1995; Pinot et al., 1995; Arand et al., 1996 and 1999; Tzeng et al., 1998; Laughlin et al., 1998). The reaction also proceeds *via* an alkyl-enzyme intermediate. Sequence alignments showed that the catalytic residues Tyr152 and Tyr215 from the epoxide hydrolase of AD1 are absolutely conserved in the soluble epoxide hydrolases from plant and mammals. The same alignments strongly indicate that both tyrosine residues are also conserved in the microsomal epoxide hydrolases from insect and mammals. Only a few residues are absolutely conserved among all epoxide hydrolases and this suggests that Tyr299 and Tyr374 of rat microsomal epoxide hydrolase and Tyr383 and Tyr464 of mouse soluble epoxide hydrolase also are catalytic residues that assist in substrate activation by donating a proton. Site-directed mutagenesis experiments should be performed to test the role of these tyrosines in the catalytic mechanisms of these enzymes.

The charge relay residue of rat microsomal epoxide hydrolase was a glutamate instead of the aspartate as present in the bacterial and soluble epoxide hydrolases.

Recently, it was postulated that the rat microsomal epoxide hydrolase also has two charge relay residues (Glu376 and Glu404) in analogy with the epoxide hydrolase from *A. radiobacter* AD1 (Tzeng et al., 1998). However, Glu376 is probably positioned in the cap domain region, since it is only separated by one residue from the absolutely conserved Tyr374 which resides in the cap domain, whereas Asp131 from the epoxide hydrolase of *A. radiobacter* AD1 is located in the main domain. The X-ray structure of the AD1 epoxide hydrolase shows that Asp131 is at hydrogen bonding distance from the general base His275. The residue in the analogous position of Glu376 in the amino acid sequence of epoxide hydrolase is Ala217, since this residue is close to the conserved and catalytic Tyr215 which aligns with Tyr374 from rat microsomal epoxide hydrolase. Ala217 is positioned far away from the catalytic His275, indicating that the observed drop in activity upon mutation of Glu376 to Gln might not result from a distortion in the charge relay system. Glu376 was also not considered as an alternative charge relay residue by Arand et al. (1999), who argued that the loss of activity with the Glu404 to Gln mutant might be due to a high proportion of misfolded mutant protein.

Haloalkane dehalogenases and epoxide hydrolases are the only  $\alpha/\beta$ -hydrolase fold enzymes that have an aspartate as the nucleophile, and this is an essential feature since the substrates of these enzymes do not have a carbonyl function. The presence of a carbonyl function in the alkyl-enzyme intermediate is required for its hydrolysis and therefore it has to be supplied by the enzyme (Hammock et al., 1994; Janssen et al., 1994). Other  $\alpha/\beta$ -hydrolase fold enzymes use either a Ser (lipases, esterases and proteinases) or a Cys (dienelactone hydrolase) as the nucleophile, since the substrates for these enzymes contain a carbonyl func-

tion, which results in ester or thioester intermediates that can easily be hydrolyzed by water.

#### Kinetic Mechanism

The kinetic mechanisms of the conversion of styrene oxide and (*R*)-*p*-nitrostyrene oxide by wild-type epoxide hydrolase from *A. radiobacter* AD1 was studied using steady-state and pre-steady-state techniques (Chapter 3). To understand which reaction steps determine the  $k_{\text{cat}}$  and  $K_m$  values and to obtain insight in the nature of the enantioselectivity, stopped-flow fluorescence and rapid quench experiments were performed to determine the kinetic mechanism and the associated rate constants for each enantiomer of styrene oxide.

The catalytic cycle for the conversion of (*R*)-styrene oxide contained four distinguishable kinetic steps, whereas only three steps could be found for the conversion of (*S*)-styrene oxide and (*R*)-*p*-nitrostyrene oxide. The catalytic schemes for both enantiomers of styrene oxide are summarized in Figure 3 together with the determined rate and equilibrium constants. The hydrolysis of (*R*)-styrene oxide proceeds *via* two covalent intermediate states (E-R1 and E-R2). The two intermediates can be observed separately since the formation of E-R1 results in a rapid decrease of the intrinsic protein fluorescence, whereas the formation of E-R2 is accompanied by a large increase of the fluorescence signal. This unimolecular isomerization step was not observed for (*S*)-styrene oxide and (*R*)-*p*-nitrostyrene oxide, indicating that it is not a common step but is rather specific for (*R*)-styrene oxide. The hydrolysis of the covalent intermediate is rate limiting for both enantiomers of styrene oxide and for (*R*)-*p*-nitrostyrene oxide. The reaction steps

that precede the hydrolysis step are much faster and as a result the hydrolysis rate solely determines the value of the steady-state  $k_{\text{cat}}$  value.

The alkylation steps of epoxide hydrolase show some interesting features. The rates for alkylating the enzyme are very high, especially when compared to the rates of the hydrolysis steps and the rate of the unimolecular isomerization step in case of (*R*)-styrene oxide (Figure 3). Furthermore, the alkylation step is reversible. The dealkylation rates and the hydrolysis rates are much lower than the alkylation rates and consequently the covalent intermediate can accumulate to a great extent. This means that when the enzyme reaction is in steady state, essentially all of the epoxide hydrolase will be alkylated. The dealkylation rate for the conversion of (*R*)-styrene oxide is 10-fold higher than that found for (*S*)-styrene oxide and (*R*)-*p*-nitrostyrene oxide, indicating that the first covalent intermediate in the catalytic cycle of (*R*)-styrene oxide is less stable than the covalent intermediate formed from (*S*)-styrene oxide and (*R*)-*p*-nitrostyrene oxide. This instability is overcome by the unimolecular isomerization step that follows, which results in a more stable covalent intermediate as can be judged from the slow back rate of this isomerization step and the low hydrolysis rate. The substrate binding constants for the enantiomers of styrene oxide are two orders of magnitude higher than the steady-state  $K_m$  values and this is explained by the extensive accumulation of the covalent intermediate. Therefore, the  $K_m$  value is indicative for the efficiency of covalent intermediate accumulation in the alkylation half-reaction, whereas the  $k_{\text{cat}}$  value describes the hydrolysis rate of the covalent intermediate in the hydrolytic half-reaction.

The  
mecha  
of the a  
These r  
proton  
epoxide  
are par  
phenolic  
the nuc  
residues  
Tyr215  
Y152F+  
construc  
mutants  
the (*R*-  
nitrosty  
compar  
 $K_m$  val  
double  
the stru  
disturbe  
residue:  
of the e  
tyrosine  
activity  
obtain l  
Stop  
solve th  
of the  
and the  
that the  
mutant

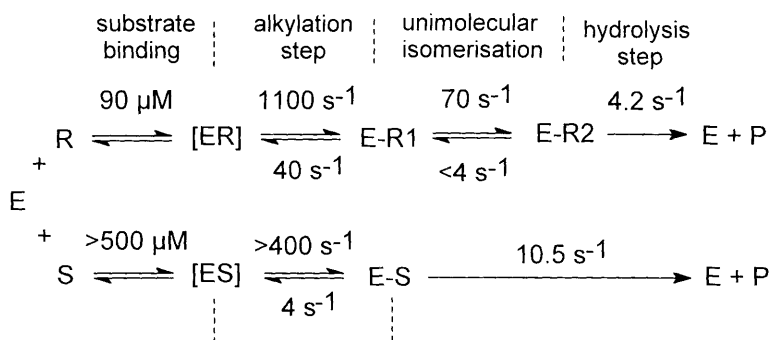


**Figure 3.** The kinetic mechanisms of epoxide hydrolase for the hydrolysis of (*R*)- and (*S*)-styrene oxide to product.

The high alkylation rates in the reaction mechanism of epoxide hydrolase are a result of the activating role of Tyr152 and Tyr215. These residues were identified as possible proton donors from the X-ray structure of epoxide hydrolase. Both tyrosine residues are part of the active site and have their phenolic hydroxyl groups pointing towards the nucleophile Asp107. To study these residues, Tyr152 was mutated to Phe and Tyr215 was mutated to Phe and Ala, and the Y152F+Y215F double mutant was also constructed. The Tyr152 and Tyr215 mutants showed that the  $k_{cat}$  values for the the (*R*)-enantiomers of styrene oxide and *p*-nitrostyrene oxide are only 2–4-fold lowered compared to wild-type enzyme, whereas the  $K_m$  values have increased a 1000-fold. The double mutant is catalytically inactive while the structural integrity of the enzyme is not disturbed, which shows that both tyrosine residues are needed for the catalytic activity of the epoxide hydrolase. Thus, at least one tyrosine residue is essential for catalytic activity, but two tyrosines are needed to obtain low  $K_m$  values.

Stopped-flow fluorescence was used to solve the rate and the equilibrium constants of the separate reaction steps of the Y215F and the Y215A mutants. The results show that the 1000-fold higher  $K_m$  values of these mutants for (*R*)-styrene oxide originate

mainly from the 15–40-fold increase of the substrate binding constant  $K_S$  and a 20-fold decreased alkylation rate  $k_2$ . The rates of hydrolysis of the covalent intermediate are not affected by these mutations and the rate of the unimolecular isomerization step and the dealkylation rate are only moderately affected. Therefore, the alkylation rates for both mutants are comparable to the rates of dealkylation and the unimolecular isomerization, which are the back and the forward reaction, respectively, and as a result the first covalent intermediate species hardly exists in the pre-steady-state experiments. The second covalent intermediate can still accumulate to some extent but only at high concentrations of (*R*)-styrene oxide. Due to the high  $K_m$  value of the Y152F mutant for (*R*)-styrene oxide the pre-steady-state kinetics could not be solved for this mutant, but the steady-state kinetic parameters are similar to those of the Tyr215 mutants and therefore similar pre-steady-state kinetics are expected for the Y125F mutant. The results clearly show that Tyr215 and Tyr152 are needed in epoxide hydrolase for substrate binding and high alkylation rates. We postulate that these tyrosine residues act as proton donor in the alkylation reaction of epoxide hydrolase as is shown in Figure 2. The actual transfer of the proton from the tyrosine to the covalent intermediate has not



been shown directly, but evidence presented in *Chapter 5* supports this conclusion.

The identification of the tyrosine residues as substrate activator and proton donor in epoxide hydrolase gives an indication about the origin of the observed quenching of the intrinsic protein fluorescence which made the pre-steady-state experiments possible. The rapid decrease in the intrinsic fluorescence of epoxide hydrolase upon mixing with substrate is not associated with the binding of the substrate in the active site but with the formation of the covalent intermediate. The protonation of the covalent intermediate by either Tyr152 or Tyr215 and the formation of this covalent intermediate are a concerted reaction. The loss of a proton by one of the tyrosine residues generates a tyrosinate, which causes quenching of tryptophan fluorescence by a mechanism that involves resonance energy transfer from the tryptophan to the tyrosinate (*Chapter 5*).

#### Enantioselectivity

Racemic styrene oxide is hydrolyzed by epoxide hydrolase with an  $E$  value of 16 and the complete conversion showed a peculiar substrate depletion pattern. The ( $R$ )-enantiomer of styrene oxide is hydrolyzed first, inhibiting the conversion of the ( $S$ )-enantiomer, which is subsequently hydrolyzed at a faster rate. The steady state  $k_{\text{cat}}$  and the  $K_m$  value of epoxide hydrolase for ( $R$ )-styrene oxide are 3-fold and 40-fold lower, respectively, than for the ( $S$ )-enantiomer, which explains the observed sequential hydrolysis since the enantiomer that is converted first has the lowest  $K_m$  value. The obtained rate constants for the reaction mechanism of styrene oxide showed that the ratio of the  $k_{\text{cat}}/K_m$  values for both enantiomers, which describes the  $E$  value, is almost identical to the ratio of the  $k_2/K_S$  values for both enantiomers. Therefore, the differences in the alkylation rates  $k_2$  and the differences in

the substrate binding constants  $K_S$  between the enantiomers of styrene oxide mainly determine the observed enantioselectivity. Furthermore, the differences in the dealkylation rates would diminish the enantioselectivity, if there was no extra unimolecular conformational change in the kinetic mechanism of ( $R$ )-styrene oxide that leads to increased capturing of the substrate.

One of the constructed epoxide hydrolase mutants has an improved enantioselectivity compared to wild-type enzyme (*Chapter 4*). The Y215F mutant has drastically changed steady-state kinetic parameters for styrene oxide and substituted variants thereof. The conversion of the ( $S$ )-enantiomer is most affected by the mutation. This resulted in a 2-fold increase of the  $E$  value of the mutant epoxide hydrolase for styrene oxide,  $p$ -nitrostyrene oxide, and  $m$ -chlorostyrene oxide, and a 4-fold increase of the enantioselectivity for  $p$ -chlorostyrene oxide. The pre-steady-state kinetics of the conversion of ( $R$ )-styrene oxide by the Y215F mutant show that  $k_2$  and  $K_S$  are the most affected kinetic parameters compared to wild-type enzyme. The alkylation rate is low but is not rate limiting. Since the hydrolysis rates are not affected in the Y215F mutant, the 15-fold decrease in the  $k_{\text{cat}}$  for ( $S$ )-styrene oxide is expected to originate from a rate-limiting alkylation step instead of a rate-limiting hydrolysis step as in wild-type enzyme. The presence of another tyrosine residue in the active site of epoxide hydrolase is essential to retain catalytic activity. Since two tyrosine residues appear to be conserved in other epoxide hydrolases as well, we expect that mutation of one of the two tyrosine residues in those epoxide hydrolases also might result in increased enantioselectivity.

#### X-ray Structure and Active Site Residues

The X-ray structure of the epoxide hydrolase from *A. radiobacter* AD1 has been determined at 2.1-Å resolution (Nar-

dini et al. 1994). The enzyme topology shows a  $\beta$ -sheet which is interrupted by two  $\alpha$ -helices in the main domain (Figure 1). The two tyrosine residues are positioned in the excursions of the  $\beta$ -sheet after  $\beta$ -strands 6 and 7. The tyrosine residues are positioned in the cap domain and the first excursions of the backbone.

The mutation of the tyrosine residues has been shown to affect the catalytic activity in this mutant (W38F and Y215F) and they have a lower  $k_{\text{cat}}$  value compared to wild-type. The  $K_m$  value of styrene oxide is almost identical to that of the wild-type, which indicates that the mutation of the tyrosine residues is the only one affected by the mutation. The reaction mechanism of the reaction, the architecture of the active site, and the mutant enzyme of Phe108 and Tyr215 also impact the proton donor.

The active site is lined by the backbone from the cap domain.

dini et al., 1999). The main domain of the enzyme has the typical  $\alpha/\beta$ -hydrolase fold topology and consists of a central parallel  $\beta$ -sheet which is flanked on both sides by 6  $\alpha$ -helices in total. The cap domain is a large excursion between  $\beta$ -strands 6 and 7 of the main domain and consists of 5  $\alpha$ -helices (Figure 1). The catalytic residues that are positioned in a hydrophobic cavity between the two domains are positioned on loops excursing from the  $\beta$ -sheet of the main domain. The nucleophile Asp107 follows after  $\beta$ -strand 5, the general base His275 after  $\beta$ -strand 8, and the charge relay residues Asp131 and Asp246 follow after  $\beta$ -strand 6 and 7, respectively. The proton donors Tyr152 and Tyr215 are supplied by the cap domain and they reside in the first and the fifth  $\alpha$ -helix, respectively.

The oxyanion hole is formed by the backbone amide atoms of Trp38 and Phe108 as shown in Figure 2. Both residues have been mutated but the results are not included in this thesis. Preliminary work on the W38F and the F108W mutants shows that they have 100-fold and 50-fold reduced  $k_{\text{cat}}$  values for (*R*)-styrene oxide, respectively, compared to wild-type enzyme, whereas the  $K_m$  value of the F108W for (*R*)-styrene oxide is hardly affected. These results indicate that the rate-limiting hydrolysis step of the catalytic cycle for (*R*)-styrene oxide is the only reaction step that is seriously affected by the mutation. The presence of an oxyanion hole is critical for the hydrolysis reaction, indicating that the precise architecture of the oxyanion hole in these mutant enzymes is distorted. The side chain of Phe108 is in a tilted-T conformation with the Tyr215, indicating that this residue is also important for the positioning of the proton donor.

The active site of epoxide hydrolase is lined by two tryptophan residues, Trp38 from the oxyanion hole and Trp183 from the cap domain region, of which Trp183 is

probably associated with the fluorescence changes observed in the stopped-flow experiments. The X-ray structure shows that the edge of the indole ring of Trp183 is positioned close to the phenolic side chains of the proton donors Tyr152 and Tyr215, which are supposed to be responsible for quenching in their deprotonated state. Preliminary stopped-flow experiments with the W183F mutant and styrene oxide shows that the characteristic fluorescence quenching, that is observed with wild-type enzyme upon hydrolysis of (*R*)-styrene oxide, is totally absent, whereas the distinctive fluorescence increase that is associated with the unimolecular isomerisation is still observable. The steady-state kinetic parameters of the W183F mutant for (*R*)-styrene oxide are comparable with those of wild-type enzyme, indicating that the fluorescence signal of Trp183 is specifically quenched when styrene oxide is covalently bound to wild-type enzyme.

In the X-ray structure, the amide side chain of Gln134 is hydrogen bonded to the side chains of the proton donors Tyr152 and Tyr215, and the nucleophile Asp107 and occupies the space where substrate is supposed to bind. This inactive form of epoxide hydrolase is the result of a crystal contact that disrupts part of the molecule (Nardini et al., 1999). The loop containing the charge relay residue Asp246 was pulled away from the active site into the solvent as a result of the crystal contact and this allowed the loop containing Gln134 to reposition near the active site. The Q134A mutant has similar steady-state kinetic parameters as wild-type enzyme and Gln134 is therefore not important for catalysis and probably does not belong in the active site of epoxide hydrolase (*Chapter 5*). Furthermore, the results of an inhibition study with unsubstituted amide molecules show that phenylacetamide binds with a high affinity in the active site of epoxide hydrolase. This

explains the apparent high affinity of Gln134 for the active site in the distorted crystal structure.

The inactive conformation of epoxide hydrolase, that is observed with X-ray crystallography, might also exist under normal assay conditions. Kinetic evidence that is presented in *Chapter 3* shows that less than 5% of the enzyme is in a conformation that is unable to bind (*R*)-styrene

oxide at the moment that substrate and enzyme are mixed. This inactive enzyme has to undergo a slow conformational change ( $1-3 \text{ s}^{-1}$ ) before it participates in the reaction. A plausible explanation for this phenomenon is that the two loops containing Gln134 and Asp246 are in constant movement in solution, allowing Gln134 to enter the active site to form a relative stable inactive conformation.

**Altschu**  
E. W.  
local  
403-4

**Andrad**  
and M  
secon  
circul  
unsup  
*Prote*

**Arand, M**  
Friedl  
B. D.  
mamr  
bacter  
other  
potent  
enzym  
**338, 2**

**Arand, M**  
H. D.,  
peroxi  
to an u  
distrib  
hydro

**Arand, M**  
Urban  
Oesch  
micros  
replac  
strong  
*J. 337,*

**Arand, M**  
(1996)  
the cat  
hydro

**Archelas**  
Synthe